processes

MDPI

Article

Chemical Composition and Reactivity of *Quercus pubescens* Bark and Bark Fractions for Thermochemical Biorefinery Applications

Umut Şen [1,*], Büşra Balcı [1], Şefik Arıcı [2], Beyza Şat [3], Isabel Miranda [4] and Helena Pereira [4]

[1] Department of Energy Systems Engineering, Izmir Institute of Technology, 35430 Gülbahce, Turkey; busrabalci@iyte.edu.tr
[2] Biomass Energy Systems and Technologies Application and Research Center, Ege University, 35100 Bornova, Turkey; sefik.arici@ege.edu.tr
[3] Department of Interior Architecture and Environmental Design, Faculty of Architecture and Design, Özyeğin University, 34794 Istanbul, Turkey; beyza.sat@ozyegin.edu.tr
[4] Centro de Estudos Florestais, Laboratório Associado Terra, Instituto Superior de Agronomia, Universidade de Lisboa, Tapada da Ajuda, 1349-017 Lisboa, Portugal; imiranda@isa.ulisboa.pt (I.M.); hpereira@isa.ulisboa.pt (H.P.)
* Correspondence: umutsen@iyte.edu.tr

Abstract

Advancing circular bioeconomy in thermochemical biorefineries requires species-specific data that link biomass composition and thermochemical performance. Here, we provide the first integrated thermochemical dataset for *Quercus pubescens* bark combining FT-IR, XRD, XRF, TGA, and measured ash fusion temperatures (AFT). The results reveal that bark is enriched in phenolic extractives (21.2%) and inorganics (15%), with calcium oxalate monohydrate (COM) dominating the inorganic fraction, as confirmed by FT-IR and XRD. Thermal decomposition occurs between 150 °C and 690 °C. Pyrolysis follows diffusion-controlled kinetics, with apparent activation energies for bark and its fractions ranging between 70 and 103 kJ mol^{-1}. Extraction increases the activation energy of bark. The ash exhibits a high AFT (softening: 1421 °C, flow: 1467 °C), placing this feedstock within the low-slagging, moderate-fouling range compared to other lignocellulosics. The observed COM-to-$CaCO_3$/CaO transformation upon heating contributes to the elevated AFT. Reactivity analyses of bark fractions support thermochemical biorefinery routing of fractions: extracted bark (EB) and desuberinised bark (DB) are highly reactive and well-suited to combustion/gasification, whereas raw bark (B) and Klason lignin (KL) exhibit higher thermal stability and yield more persistent char, favoring slow pyrolysis for biochar production. Such routing strategies optimize energy recovery and also enable co-products with environmental co-benefits.

Keywords: biorefinery; bark; *Quercus pubescens*; activation energy; ash fusion temperature; suberin; extractives; soil management

check for updates

Academic Editor: Francesca Raganati

Received: 9 October 2025
Revised: 27 October 2025
Accepted: 27 October 2025
Published: 30 October 2025

Citation: Şen, U.; Balcı, B.; Arıcı, Ş.; Şat, B.; Miranda, I.; Pereira, H. Chemical Composition and Reactivity of *Quercus pubescens* Bark and Bark Fractions for Thermochemical Biorefinery Applications. *Processes* **2025**, *13*, 3484. https://doi.org/10.3390/pr13113484

Copyright: © 2025 by the authors. Licensee MDPI, Basel, Switzerland. This article is an open access article distributed under the terms and conditions of the Creative Commons Attribution (CC BY) license (https://creativecommons.org/licenses/by/4.0/).

1. Introduction

Quercus pubescens Willd., commonly referred to as pubescent oak or downy oak, is a sun-loving and heat-adapted oak species. It is a medium-sized tree that can be deciduous or semi-deciduous with a characteristic velvety pubescence covering leaves, buds, and shoots [1]. The species is widely distributed across central and southern Europe, from northern Spain to southern Ukraine, as well as in Anatolia and along the Caspian Sea coast [2–4]. In France and Italy, *Q. pubescens* usually forms nearly pure forests, whereas in other parts

of its range it commonly grows mixed with other oaks [3,5]. In the Mediterranean basin, the species grows up to 1300 m altitude [2]. In Turkey, *Q. pubescens* usually grows as a small tree up to 10 m in height, widespread across the country with the exception of the southeastern regions, and develops in mixed stands with *Quercus cerris* and *Pinus nigra* in altitudes up to 1700 m [1,6]. Taxonomically, *Q. pubescens* is a member of the Fagaceae family and is included in the "white oaks" group [7]. Hybrids of *Q. pubescens* are quite common, in particular with *Q. petraea*, *Q. infectoria*, and *Q. machranthera* subsp. *syspirensis* [1].

Q. pubescens wood is primarily used as firewood and not generally utilized for industrial wood production due to its irregular fiber distribution and crookedness of the trunk, as well as its high shrinkage and a tendency to crack [3,5]. The formation of a tylosis barrier hinders the penetration of chemicals into the wood, making treatment more difficult [5]. Anatomically, *Q. pubescens* wood is a ring porous wood which is quite similar to other oak woods [5,8].

However, *Q. pubescens* wood has a high extractive content [5], which imparts a notable durability with its heartwood being classified among the most durable wood species [9]. The heartwood of *Q. pubescens* wood contains up to 20% extractives that are predominantly hydrophilic compounds [9]. Possibly, due to the favorable durability properties, *Q. pubescens* wood has found application in the production of railway sleepers and, although less commonly, it was also used for carpentry and boat building barrels [10].

Q. pubescens wood has attracted interest in enology for wine barrels due to its elevated extractive content. Comparative wine-aging studies have evaluated *Q. pubescens* wood alongside *Q. petraea*, which is the traditionally preferred wood for wine color stabilization, spontaneous clarification, and structured aroma [10]. The aged wine samples from *Q. pubescens* barrels contained a higher amount of resveratrol and a lower amount of tannins than those from *Q. petraea* barrels [10,11]. Wine samples aged with *Q. petraea* chips contained a higher concentration of vanillin, whereas those aged with *Q. pubescens* chips contained a higher concentration of furan compounds, eugenol, and trans-β-methyl-γ-octalactone [11].

The phenolic extracts of *Q. pubescens* bark also attracted interest regarding their bioactivity because of antioxidant and antibacterial properties [12]. In Italy, the bark of young branches of *Q. pubescens* has already been commercialized to produce hydroethanolic extracts (*tintura madre*) for herbal medicine to treat digestive issues, skin problems, respiratory symptoms, etc.

Despite the present growing interest in utilizing lignocellulosic biomass for biorefinery applications, barks only recently started to be valued as a resource [13–15]. In general, oak barks are known to be rich in phenolic compounds, lignin, and minerals such as calcium, which make them promising feedstocks for thermochemical processes [16]. These components can be converted into a wide range of value-added products, including antioxidants, antimicrobial agents, biochars, activated carbons, and solid catalysts. The bark of *Quercus pubescens* has not been previously studied in this context. The aim of this study is to provide the first detailed chemical and thermal characterization of *Q. pubescens* bark and evaluate its potential for thermochemical biorefinery applications.

2. Materials and Methods

2.1. Sampling

The bark samples of *Q. pubescens* mature trees with 40 years of age were collected from Ivrindi Province of Balıkesir city in the Northwestern part of Turkey. The sampling area is located at 39°36′31″ N, 27°26′42″ E with 230 m altitude, and has a mean annual 628 mm rainfall and 13.4 °C temperature. The climate of the sampling area is classified as a Csa (Hot-summer Mediterranean climate) according to the Köppen climate classification. The relative humidity is lowest in July (53.95%) and highest in December (83.71%). On average,

August has the fewest rainy days (1.57 days) and December has the highest rainy days (11.40 days) (Figure 1).

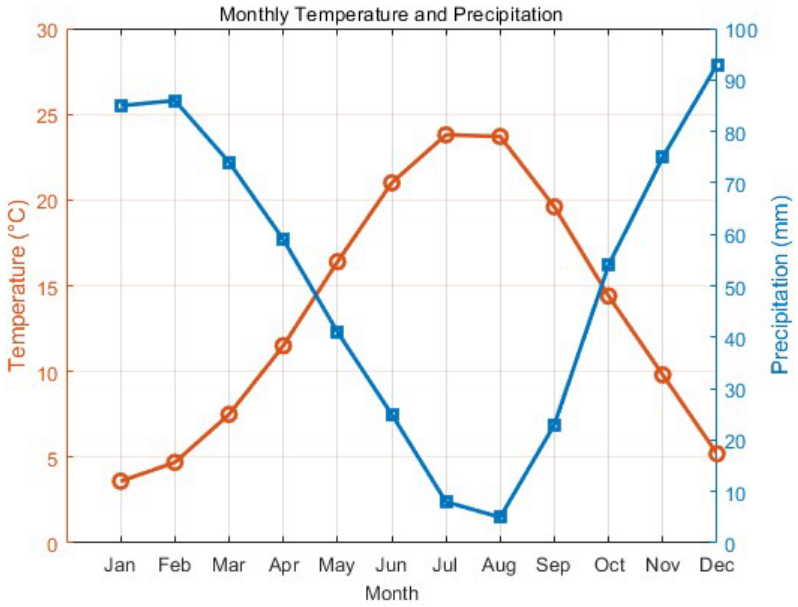


Figure 1. Walter–Lieth climate diagram of the *Quercus pubescens* sampling site.

The collected bark samples were air-dried at 20 °C for 48 h and then ground using a cutting mill to pass through a 250–420 µm sieve. The powdered samples were stored in airtight containers until further analysis.

2.2. Structural and Chemical Characterization

The structural characterization of the bark included scanning electron microscopy observations, X-ray diffraction analysis, and FT-IR analysis. The chemical characterization of the bark included a summative wet chemical analysis and mineral composition.

2.2.1. Scanning Electron Microscopy

The scanning electron microscopy (SEM) observations were carried out on granulated bark samples of 250–420 µm size. A Hitachi S2400 (Hitachinaka, Ibaraki, Japan) electron microscope was used under an accelerating voltage of 20.0 kV. The energy dispersive spectroscopic analysis (EDS) was also carried out on the same samples using a silicon drift detector.

2.2.2. X-Ray Diffraction Analysis

XRD analysis was conducted using a Bruker D8 ADVANCE (Bruker AXS GmbH, Ettlingen, Germany) diffractometer with Cu Kα radiation (λ = 1.5406 Å) operating at 40 kV and 30 mA. The scans were recorded over a 2θ range of 5–80° with a step size of 0.02° and a scan speed of 0.1°/s. The presence of calcium oxalate was confirmed by identifying characteristic peaks at 14.9°, 15.3°, 24°, 30.1°, 38.2° 2θ for calcium oxalate monohydrate (COM) [17].

2.2.3. FT-IR Analysis

The bark samples were sieved, and the fraction with particles under 180 µm was oven dried at 105 °C for 1 h prior to analysis. FTIR-ATR reflectance spectra were acquired with a Perkin Elmer Spectrum Two mid-infrared FT-IR spectrometer (PerkinElmer® GC Instruments, Rodgau, Germany) in the range of 4000–400 cm^{-1} with a spectral resolution of 8 cm^{-1}.

2.2.4. Chemical Analysis and Fractionation

The wet chemical composition (ash, extractives, suberin, and lignin) of bark (B) was determined using previously dried samples (overnight at 60 °C followed by 100 °C for 2 h). Ash content was determined by isothermally incinerating 2 g of bark in an oven at 550 °C overnight (16 h). Total extractive content was determined by three successive Soxhlet extractions according to TAPPI Standards (T204 om-88 [18] and T207 om-93 [19]) with dichloromethane (CH_2Cl_2-DCM), ethanol (C_2H_5OH-EtOH), and water (H_2O) extractions during 6 h, 18 h, and 18 h extraction time for each solvent, respectively. The extractive-free bark sample is termed here as extracted bark (EB).

The suberin content was determined by methanolysis on the previously extracted material [20]. A 1.5 g extractive-free sample was refluxed with 100 mL of a 3% methanolic solution of NaOCH3 for 3 h, filtered, and washed with methanol. The residue was refluxed with 100 mL CH_3OH for 15 min and filtered again. The filtrates were combined and acidified to pH 6 with 2 M H_2SO_4 and evaporated to dryness. The residue was suspended in 50 mL water, and the alcoholysis products were recovered with CH_2Cl_2 in three subsequent liquid–liquid extractions, with 50 mL CH_2Cl_2. The extracts were dried over anhydrous Na_2SO_4, the solvent was evaporated, and the concentrate was kept for compositional analysis. The aqueous phase was kept for analysis of glycerol. The bark fraction after extraction and suberin removal is here termed as desuberinised bark (DB).

The Klason (KL) and acid-soluble lignin contents were determined according to TAPPI T222 om-88 [21] and TAPPI UM 250 Standards [22] on the previously extracted and desuberinised samples. H_2SO_4 (72%, 3.0 mL) was added to 0.35 g of the material, the mixture was placed in a water bath at 30 °C for 1 h, and then diluted to a concentration of 4% H_2SO_4 and hydrolyzed for 1 h at 120 °C [23]. The Klason lignin (KL) fraction obtained after the sequential extractions and acid hydrolysis represents an acid-insoluble condensed residue that does not represent native lignin since it is known that lignin undergoes partial condensation and dehydration during hydrolysis. The Kason lignin was analyzed in this study as a reference material for the thermochemical behavior of the recalcitrant lignin-derived matrix, not as native lignin itself. This approach was selected for its applicability in thermochemical biorefineries.

Polysaccharide content was estimated by mass difference to 100%.

Ratios of polysaccharides-to-lignin and of suberin-to-lignin were calculated since they give insight into the thermal stability of the material.

2.2.5. XRF Analysis

The inorganic composition of *Q. pubescens* bark was determined through an X-ray fluorescence analyzer (Niton XL 3t, Thermofisher Scientific, Waltham, MA, USA). The tests were conducted in triplicate, and the results were presented as average values.

The mineral composition of the bark was converted to its oxide form to evaluate its fouling risk.

2.3. Thermochemical Characteristics

Thermochemical characteristics of *Q. pubescens* bark (B) and its three fractions of extracted bark (EB), desuberinised bark (DS), and Klason lignin (KL) were analyzed by thermogravimetric analysis.

2.3.1. Thermogravimetric Analysis

The thermogravimetric analysis was conducted with TA Instruments SDT 2960 simultaneous DSC-TGA analyzer (TA Instruments, New Castle, DE, USA) using alumina pans under air or nitrogen flow rates between 20 and 50 mL min^{-1}. For the thermogravimetric

analyses, a linear 4-step heating program was applied: in the first step, approximately 5 mg of the samples were kept isothermally at 30–40 °C for 5–10 min; a heating step followed until 800 °C with heating rate of 10 °C min^{-1}; in the third step, the samples were kept isothermal for 10 min at 800 °C; in the last step, the samples were cooled to ambient temperature with a cooling rate of 50 °C min^{-1}.

The burnout temperature (T_b) was calculated using the conversion method at 99% conversion using thermogravimetric (TG) curves [24]. The temperature at maximum degradation rate (T_m) was obtained from the differential thermogravimetric (DTG) curves.

2.3.2. Pyrolysis Kinetics

A solid-state reaction rate is dependent on both conversion (α) and temperature (T):

$$\frac{d\alpha}{dt} = A \times e^{-\frac{Ea}{RT}} \times f(\alpha) \quad (1)$$

The temperature dependence of the reaction is calculated using the Arrhenius equation, where A (s^{-1}) is the pre-exponential factor, E_a is the activation energy (kJ mol^{-1}), and R is the universal gas constant (8.314462 J mol^{-1} K^{-1}). Under linear heating conditions, Equation (1) can be written by introducing the heating rate β (dT/dt).

$$\frac{d\alpha}{dT} = \frac{A}{\beta} \times exp^{-\frac{Ea}{RT}} \times f(\alpha) \quad (2)$$

The integral form of this equation (Equation (3)) is written as follows:

$$g(\alpha) = \int_0^{\alpha} \frac{d(\alpha)}{f(\alpha)} = \frac{A}{\beta} \int_{T0}^{T} exp^{-Ea/RT} \times dT \quad (3)$$

Numerical methods are required to calculate the kinetic parameters (E_a and A). In the present study, the Coats–Redfern method with different kinetic models (first-order, Avrami–Erofeev A2, and Jander diffusion models) was tested for the best coefficient of determination values [25].

The kinetic parameters were determined exclusively under an inert (N_2) atmosphere to describe the intrinsic devolatilization behavior of *Q. pubescens* bark and its fractions, without interference from oxidative reactions. Conversely, thermogravimetric measurements conducted under air were used qualitatively to evaluate specific combustion characteristics, providing complementary insight into the combustion reactivity and ash behavior of bark and bark fractions under practical thermochemical conditions.

2.3.3. Solid Fuel Characterization

The higher heating value (HHV) of the bark sample was determined using a bomb calorimeter (Parr 6300, Parr Instrument Company, Moline, IL, USA), following the procedure outlined in ASTM D5865-13. Between 0.5 and 1.0 g of oven-dried and homogenized sample was pressed into a pellet and combusted in an oxygen-rich atmosphere at 30 bars. The resulting temperature rise in the surrounding water jacket was used to calculate the HHV. All measurements were performed in at least three replicates, and the mean value was reported.

Proximate analysis was conducted to determine the moisture content, volatile matter, ash content, and fixed carbon following standard methods. Moisture content was determined by drying the sample at 105 °C for 24 h in accordance with ASTM E871-82 [26]. Volatile matter was measured by heating the dried sample at 950 °C for 7 min in a covered crucible (ASTM E872-82 [27]). Ash content was determined by combusting the sample at

575 °C for 4 h in a muffle furnace as per ASTM D1102-84 [28]. Fixed carbon was calculated by mass difference. All analyses were conducted in six replicates.

2.4. Slagging and Fouling Behavior

Ash fusion behavior was evaluated using a muffle furnace equipped with visual inspection according to U-Therm YX-HRD 3000, Xiangtan, China. Ash residues obtained from the proximate analysis were shaped into pyramids using a sucrose solution (10%) and heated at a controlled rate up to 1500 °C under an oxidizing atmosphere. The characteristic ash melting temperatures were recorded: shrinkage temperature (ST), deformation temperature (DT), hemispherical temperature (HT), and flow temperature (FT). Observations were made at intervals using a high-temperature camera or optical access.

Ash fouling behavior was evaluated by determining ash deformation temperature as well as using total alkali content and bed agglomeration index as indicators.

3. Results and Discussion

3.1. Structural Characterization

SEM observations of the *Q. pubescens* powdered bark reveal a fragmented, plate-like surface with angular fracture planes, a morphology consistent with brittle phloem and cork cells that fracture and originate cellular and cell wall fragments (Figure 2). The anatomical analysis of *Q. pubescens* bark, described in detail by Lavrič et al. [29], indicates the formation of early and late phloem in agreement with our SEM results. Cork cells from the periderms could be observed, which suggests that the bark forms a rhytidome (Figure A1) [12]. Several inorganic crystals are observed, presumably in sclereid cells between the cork and phloem cells. The presence of calcium is confirmed from the SEM and EDS results (Figures 2 and A1). These results agree with previous publications and indicate that the inorganic composition of oak barks is dominated by calcium [16,30]. The inorganic composition of *Q. pubescens* bark seems to be similar to that of *Q. cerris* and *Q. vulcanica* [31,32].

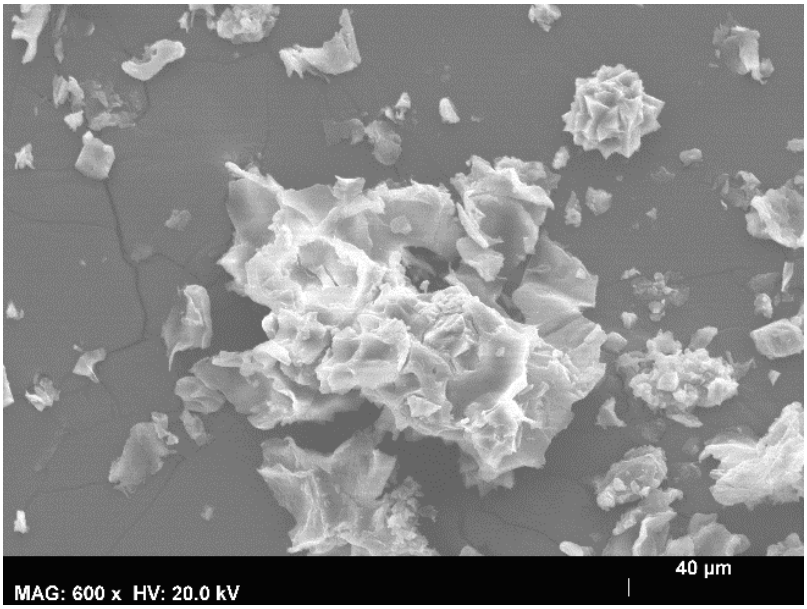


Figure 2. SEM micrograph of *Quercus pubescens* bark.

The inorganic composition of *Q. pubescens* bark was further analyzed with X-ray diffraction (XRD) analysis to better understand the inorganic composition, in particular regarding the calcium oxalate types. The results of XRD analysis are shown in Figure 3.

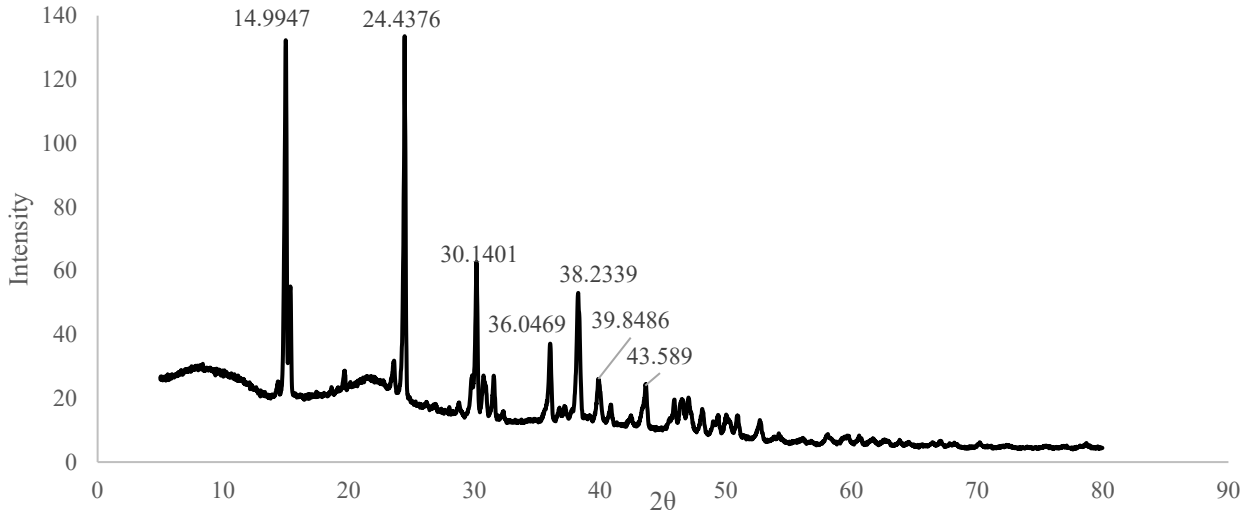


Figure 3. Powder X-ray diffractogram (Cu Kα) of *Quercus pubescens* bark. Strong peaks at 14.9°, 24.4°, and 30.1° 2θ correspond to calcium oxalate monohydrate (COM). A weak cellulose-I (200) signal near 22–23° is overlapped by the strong COM line. The broad hump at 15–22° indicates the amorphous hemicellulose/lignin matrix.

The diffractogram of *Quercus pubescens* bark exhibits a mineral-dominated pattern superimposed on the broad amorphous hump typical of lignocellulosic materials (approximately 15–22° 2θ). Very intense reflections at 14.9°, 24.4°, and 30.1° 2θ indicate abundant calcium oxalate monohydrate (whewellite) [33], a well-known mineral in oak barks [31].

A weak cellulose-I signal is discernible near 22–23° 2θ [34] but is strongly overlapped by the adjacent calcium oxalate monohydrate peak at 24.4°. Additional reflections at 26.6° and 29.4°, 39.4°, and 43.1° 2θ possibly correspond to other minerals. The pattern confirms that native crystalline cellulose is present, but its intensity is suppressed by the high load of mineral crystallites.

No distinct peaks at 14.3°, 20.1°, or 32.2° 2θ were detected, suggesting that weddellite (COD) is absent or present only in trace quantities [33]. These results highlight the predominance of calcium oxalate monohydrate in the bark matrix, a feature that possibly influences its thermochemical performance, such as reducing its activation energy [35] as well as char transformation and tar reforming [36].

3.2. Chemical Composition

The chemical composition of bark is a key parameter for its evaluation as a feedstock in thermochemical biorefineries because it indicates the possible product yields. *Q. pubescens* bark is dominated by a high amount of inorganic matter (15%) and of extractives 21%) (Table 1). Polar extractives solubilized in ethanol and water, probably phenolic extractives, make up approximately 90% of the total extractives, which is one of the highest extractive yields among different bark species, in particular oak barks [37].

The estimated polysaccharide content of the bark is low (approximately 35%), and lignin content (24%) is similar to that of hardwoods [16]. Suberin is also a chemical component (4%) in agreement with the presence of cork cells (Figures 2 and A1). Although *Q. pubescens* is not a cork-rich bark, its suberin content is comparatively significant [38].

The polysaccharides/lignin ratio of 1.49 indicates a comparatively lignin-rich bark and therefore, enhanced thermal stability. Suberin confers strong barrier and carbon-retaining properties, promoting the formation of hydrophobic biochars. The suberin/lignin ratio of 0.17, although low in comparison with that of cork only (e.g., 2.0 in *Q. suber* and 1.3–1.4 in *Q. variabilis*), is indicative of the presence in this bark of the thermally resistant suberin [31,38].

Table 1. Summative chemical composition of *Quercus pubescens* bark.

Chemical Components	Dry Mass (%)	Ash-Free Mass (%)
Ash	15.03 ± 1.99	-
DCM extractives	2.00 ± 0.30	2.4
EtOH extractives	9.96 ± 0.48	11.7
H_2O Extractives	9.24 ± 0.25	10.9
Total extractives	21.20 ± 1.23	24.9
Suberin	4.07 ± 0.73	4.8
Klason lignin	21.02 ± 2.04	24.7
Acid-soluble lignin	2.99 ± 0.29	3.5
Total lignin	24.01 ± 2.33	28.3
Polysaccharides/lignin ratio	1.49	
Suberin/lignin ratio	0.17	

The inorganic elemental composition of *Q. pubescens* bark, shown in Table 2, is quite similar to that of other oak barks such as *Q. vulcanica* [32]. Calcium is the major element and is accompanied by significant amounts of magnesium and potassium. Manganese is the major minor element, and copper, as well as zinc, are present in small quantities.

Table 2. Inorganic elemental composition of *Quercus pubescens* bark.

Major Elements	Composition (mg kg^{-1})	% Major Elements
Na	108.9	0.2
K	647.9	1.1
Ca	55,023.9	96.1
Mg	753.5	1.3
P	152.4	0.3
S	294.4	0.5
Fe	96.3	0.2
Oligoelements	Composition (mg kg^{-1})	% Oligoelements
Cu	8.9	5.3
Zn	3.9	2.3
Mn	154.9	92.4
Total	57,244.9	100.0
Oxides	Composition (mg kg^{-1})	% Oxides
CaO	76,987.2	95.7
K_2O	780.9	1.0
Na_2O	146.9	0.2
MgO	1249.4	1.6
P_2O_5	349.4	0.4
Fe_2O_3	137.7	0.2
SO_3	734.6	0.9

Calcium, magnesium, and potassium oxides make up approximately 98.3% of all oxides in the bark.

The bark chemical composition was further evaluated by FTIR analysis (Figure 4). The broad absorption at 3347 cm^{-1} and the band at 2931 cm^{-1} were attributed to O–H stretching and aliphatic C–H vibrations in suberin and lignin, while the signal at 1622 cm^{-1} corresponded to aromatic skeletal vibrations and conjugated carbonyls, consistent with the high phenolic content of the bark. The weak peak around 1737 cm^{-1} indicates the presence of C=O in the ester bonds of suberin, in agreement with its low content. The strong band at 1037 cm^{-1} indicated C–O–C stretching of polysaccharides (cellulose and hemicelluloses), whereas features at 780 cm^{-1} reflected aromatic out-of-plane bending vibrations of calcium oxalate. The absorption near 516 cm^{-1} is assigned to metal–oxygen stretching, in line with the Ca–O bonding expected for oxalates and carbonates (Table 3) [31]. The concordance of FTIR and XRD thus establishes COM as the dominant inorganic phase in the lignocellulosic matrix.

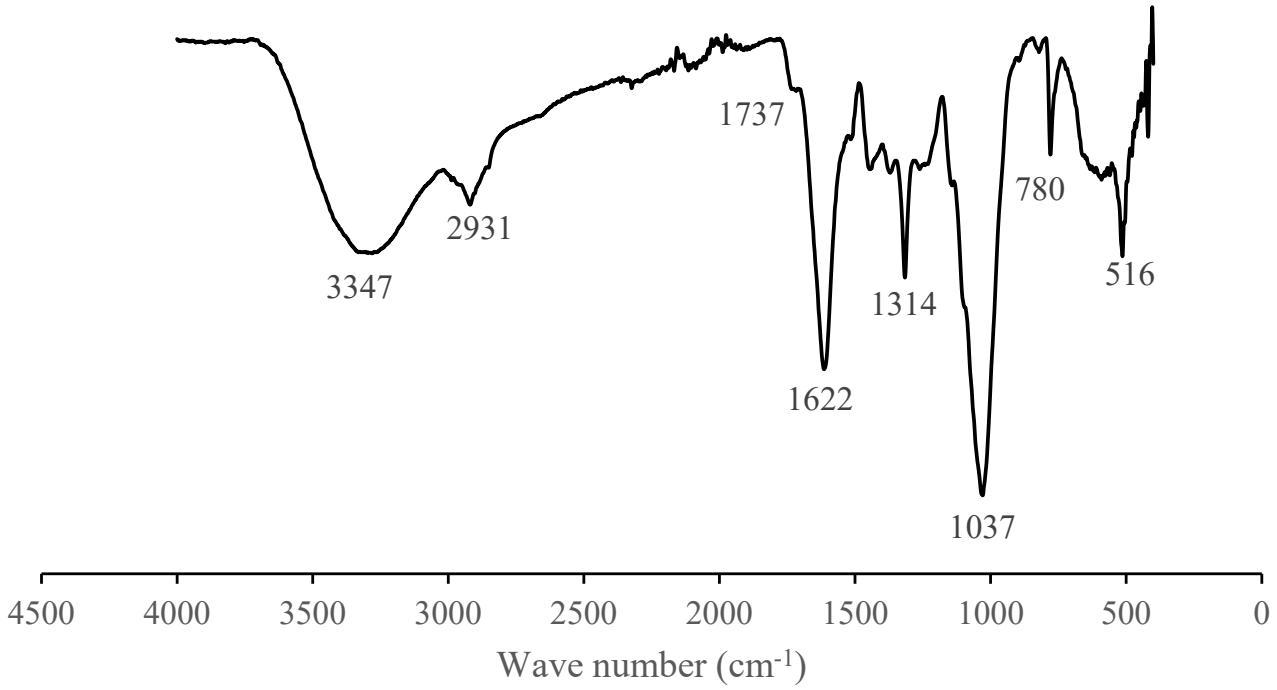


Figure 4. FT-IR spectrum of *Quercus pubescens* bark.

Table 3. Assignments of major FTIR spectral peaks of *Quercus pubescens* bark.

Wavenumber (cm^{-1})	Assignment	Functional Group and Origin
3347	O–H stretching (broad)	Hydroxyl groups in cellulose, hemicellulose, lignin, and absorbed water
2931	C–H stretching	Aliphatic chains in lignin side groups and suberin aliphatics
1737	C=O	Ester bonds in suberin
1622	C=O stretching/aromatic skeletal vibration	Conjugated carbonyls and aromatic rings in lignin and phenolic extractives; bound water bending
1314	C–H deformation/O–H bending	Cellulose and lignin structural vibrations; phenolic groups

Table 3. *Cont.*

Wavenumber (cm^{-1})	Assignment	Functional Group and Origin
1037	C–O–C stretching	Polysaccharide (cellulose and hemicellulose) glycosidic linkages
780	Aromatic C–H out-of-plane bending	Aromatic rings (lignin/phenolics); C–C/C–O deformation in calcium oxalate monohydrate
516	M–O stretching	Ca–O (calcium oxalate), possible other inorganic mineral vibrations

3.3. Thermochemical Behavior

The thermochemical behavior was assessed by pyrolysis and combustion behaviors of the raw bark (B) and its three fractions, namely extracted bark (EB), desuberinised bark (DB), and Klason lignin (KL) (Table 4, Figure A2). The pyrolysis behavior and kinetic parameters were calculated to describe inert thermal decomposition mechanisms, while the combustion data were used qualitatively to evaluate the energy utilization potential and ash performance of the bark fractions.

Table 4. Thermogravimetric data of *Quercus pubescens* pyrolysis.

	Water Loss Region (40–120 °C)		**Low-Temperature Mass Loss Region (40–210 °C)**		**Main Mass Loss Region (210–405 °C)**			**Char Mass Loss Region (405–740 °C)**		**Residual Char**
	Mass loss (%)	T_{max} (°C)	Mass loss (%)	T_{max} (°C)	Onset (°C)	Mass loss (%)	T_{max} (°C)	Mass loss (%)	T_{max} (°C)	Mass (%)
B	5.1	81.8	8.4	163.4	211.7	34.9	346.5	22.8	718.4	30.8
EB	3.4	68.7	6.2	150.8	224.0	41.6	366.9	27.1	687.6	14.8
DB	3.3	74.6	6.7	157.1	234.3	34.4	323.2	29.8	684.3	12.3
KL	3.9	73.7	5.2	73.7	223.9	23.9	349.8	32.4	627.3	30.4

B: bark, EB: extracted bark, DB: desuberinised bark, KL: Klason lignin.

3.3.1. Pyrolysis Behavior

Pyrolysis of *Q. pubescens* bark proceeds in four major stages: moisture loss, low temperature mass loss, main mass loss, and char mass loss regions (Table 4) with raw bark and bark fractions showing distinct mass loss patterns (Figure 5).

The pyrolysis behavior of *Q. pubescens* bark showed that the bark is a highly reactive material. It undergoes degradation at temperatures as low as 150 °C, which possibly corresponds to degradation of extractives and hemicelluloses, and the thermal degradation continues until 690 °C. The residual char content (30.8%) and the thermal stability of bark at high temperatures are noteworthy.

Extracted bark shows lower mass loss in the low-temperature mass loss region, which is consistent with its absence in extractives, but it has the highest amount of mass loss in the main mass loss region (41.6%). The residual char content is almost half of the raw bark, indicating a higher activity. Desuberinised bark originated the lowest amount of char, indicating another high activity. These results show that extractives and suberin contribute to the heat resistance of biomass by providing physical barriers, in agreement with a previous publication on the thermal behavior of suberin-rich cork [39].

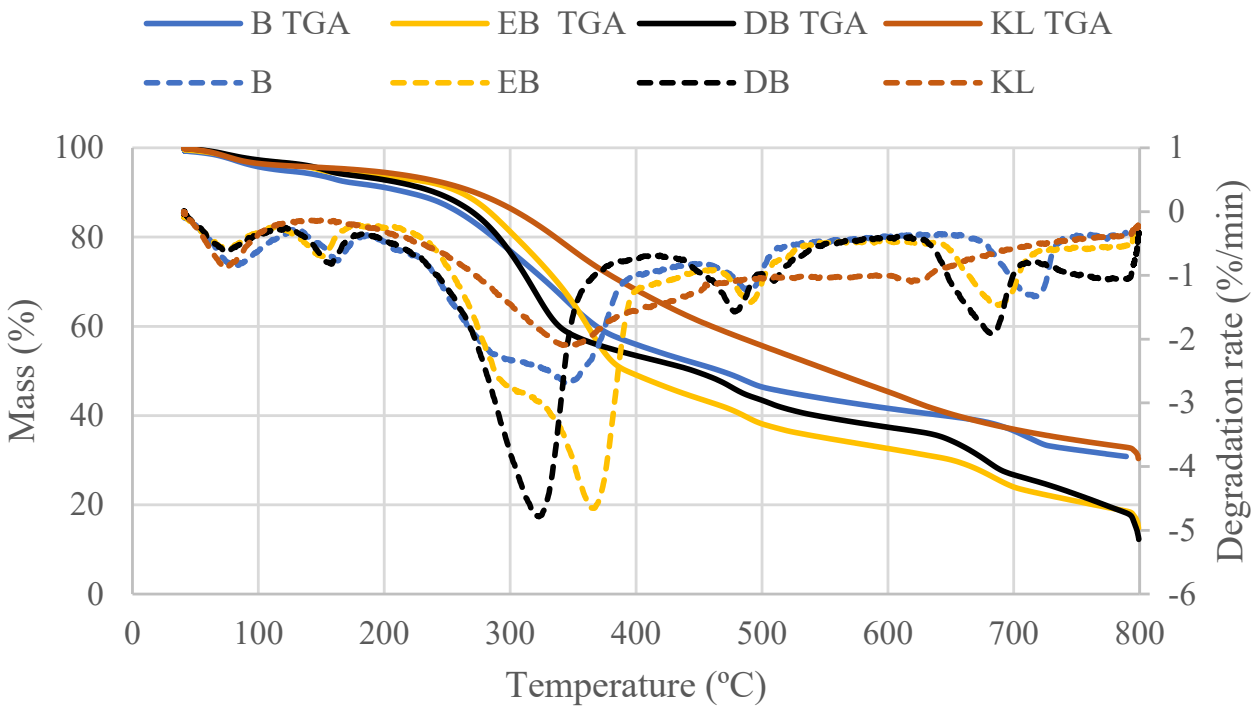


Figure 5. Pyrolysis of *Quercus pubescens* bark fractions (HR:10 °C min^{-1}). Bark fractions show different thermal degradation patterns compared to raw bark. B: bark, EB: extracted bark, DB: desuberinised bark, KL: Klason lignin.

Klason lignin produced the highest amount of char, which is consistent with its condensed structure. Interestingly, it also showed the lowest T_{max} value (627 °C) in the char mass loss region.

Kinetic modeling with the Coats–Redfern method showed that all samples followed the Jander equation (3D diffusion model) with excellent coefficient of determination (R^2) values, indicating that thermal decomposition is controlled by diffusion of volatile products through the bark matrix as the reaction progresses. Apparent activation energies (E_a) were relatively narrow, ranging from 70 to 103 kJ mol^{-1}, with raw bark (B) exhibiting the lowest barrier and extracted bark (EB) the highest (Table 5). This consistency across fractions suggests that, despite compositional differences, their thermal decomposition can be generally described by a diffusion-controlled process, emphasizing the role of the bark matrix and char residues in limiting mass transport during degradation. The apparent activation energies of *Q. pubescens* bark and bark fractions agree with those previously reported for other barks, including fir (*Abies sibirica*), larch (*Larix sibirica*), spruce (*Picea obovata*), and pine (*Pinus sibirica*) [40].

Table 5. Kinetic analysis of *Quercus pubescens* bark pyrolysis.

	Apparent E_a (kJ/mol)	A (1/s)	R^2	Best-Fit Kinetic Model
B	69.88	1.93×10^5	0.9926	Jander
EB	103.25	7.86×10^7	0.9880	Jander
DB	87.53	3.97×10^6	0.9732	Jander
KL	98.57	1.74×10^7	0.9873	Jander

B: bark, EB: extracted bark, DB: desuberinised bark, KL: klason lignin.

The higher activation energy of the extracted bark fraction compared to the raw bark agrees with previous studies with *Pinus sylvestris* var. *mongolica*, *Fraxinus mandschurica*, and *Eucalyptus grandis* × *E. urophylla* woods, where the presence of extractives enhanced the decomposition of the wood structural components [41,42]. Phenolic extractives can act catalytically, favoring the formation of acids while inhibiting the formation of levoglucosan, the main anhydro sugar formed from cellulose depolymerization, which results in different volatile and char yields in pyrolysis [41].

Another explanation for the higher activation energy in EB is the removal of soluble salts during the extraction process, which may act as catalysts. Fetisova et al. (2023) showed that bark treated with KCl and K_3PO_4 had significantly reduced apparent activation energy [40]. On the other hand, a decrease in the apparent activation energy was also reported for extracted *Eucalyptus robusta* wood [43], suggesting that this trend may depend on the extractive composition of the specific biomass.

Desuberinised bark (DB) is more reactive than extracted bark (EB) with slightly lower activation energy (87.5 kJ/mol) and much lower frequency factor (fewer collisions are required compared to EB). The apparent activation energy of the DB is lower than B because catalytic organic extractives and part of the inorganic salts are removed during the extraction.

Interestingly, Klason lignin (KL) had a relatively high E_a and a high frequency factor (A), suggesting complex decomposition with a number of bond-breaking events. KL is recalcitrant, degrading slowly, and producing a higher char yield.

The results imply that raw bark and its Klason lignin fraction are suitable for the slow pyrolysis process to produce biochars with elevated char yields and high thermal stability, as discussed in the following section. On the other hand, extracted bark and desuberinised bark are well-suited for combustion and gasification applications with their comparatively lower char yields and higher reactivity.

Compared with combustion, gasification not only reduces the excess heat produced during combustion but also enables the production of synthetic fuels via Fischer-Tropsch synthesis. Biomass and biomass-derived wastes, including barks and black liquor, are currently being investigated, particularly for gasification to use their favorable characteristics such as intrinsic hydrogen content and alkaline properties, which increase hydrogen content in the synthesis gas, a key parameter in Fischer-Tropsch synthesis [44].

3.3.2. Combustion Behavior and Fuel Properties

The combustion characteristics of the bark fractions showed significant differences depending on chemical composition (Figure 6, Table 6). The raw bark (T_m = 325.7 °C; Tb = 691.8 °C) displayed a balanced thermal degradation pattern, with a moderate maximum degradation temperature (T_m) and a high burnout temperature (T_b), reflecting the thermal degradation of volatile components (hemicelluloses, extractives) and lignin-derived char that extends oxidation to higher temperatures.

On the other hand, the extracted bark (T_m = 328.3 °C; T_b = 662.7 °C) exhibited a slightly higher maximum degradation temperature but a lower burnout temperature, indicating a faster combustion process.

The desuberinised bark (containing only lignin and polysaccharides) (T_m = 301.3 °C; T_b = 684.5 °C) had a maximum degradation temperature at the lowest temperature among the other fractions, demonstrating that removal of suberin reduces structural resistance and promotes volatile release at lower temperatures. The relatively high burnout temperature reflects its lignin content. Thus, this fraction is the most reactive fraction in combustion.

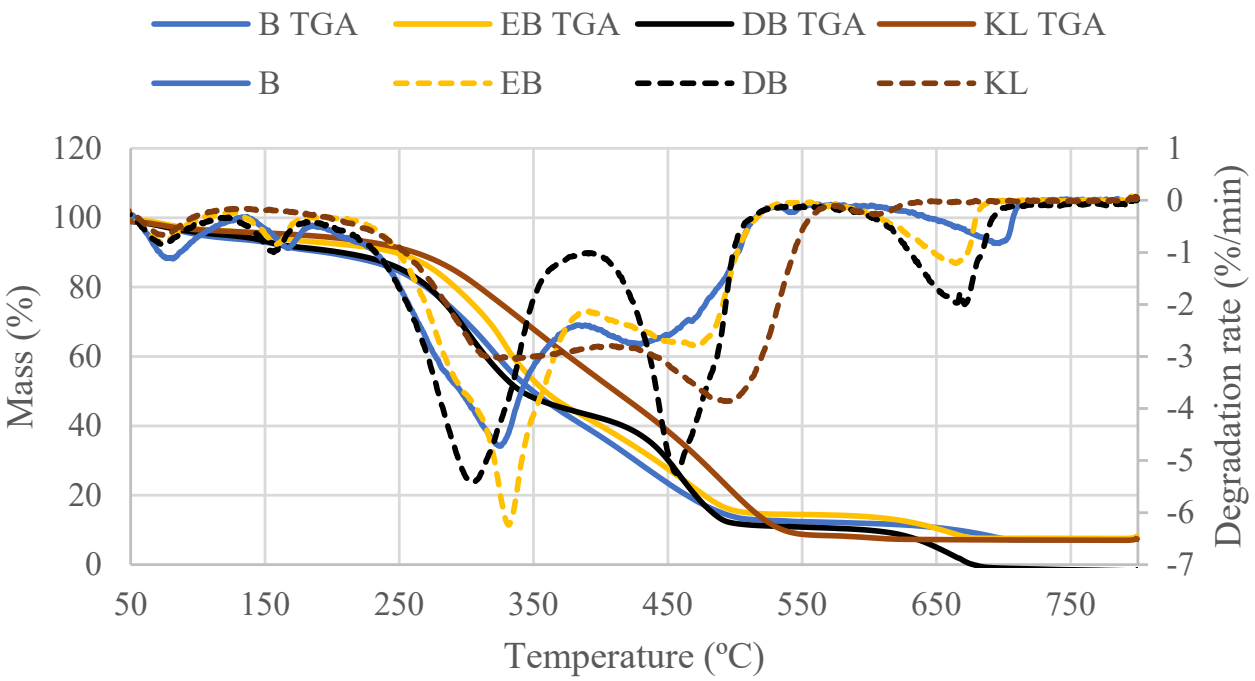


Figure 6. Combustion of *Quercus pubescens* bark fractions. Extracted and desuberinised barks show faster thermal degradations (HR:10 °C min^{-1}). B: bark, EB: extracted bark, DB: desuberinised bark, KL: Klason lignin.

Table 6. Specific combustion temperatures (°C) of *Quercus pubescens* bark fractions.

	T_m (°C)	T_b (°C)
B	325.7	691.8
EB	328.3	662.7
DB	301.3	684.5
KL	493.1	568.5

B: bark, EB: extracted bark, DB: desuberinised bark, KL: Klason lignin.

By contrast, the Klason lignin fraction (T_m = 493.1 °C; T_b = 568.5 °C) behaved differently: the maximum degradation temperature was strongly delayed due to lignin's condensed aromatic structure, but burnout occurred more rapidly (lower T_b). This result indicates that lignin-rich materials resist combustion but yield char that oxidizes more abruptly once decomposition is initiated.

The combustion properties of *Q. pubescens* bark were further analyzed by solid fuel characterization (Table 7). Proximate analysis revealed that the bark contained moderate moisture content (MC = 7.8%), which is within acceptable limits for thermochemical processing without extensive pre-drying. However, the ash content was relatively high (16.3% as-received; 17.7% dry basis), consistent with the chemical analysis results (Table 1). This high ash fraction is a significant parameter for both combustion and pyrolysis since it not only dilutes the energy content but also influences slagging and fouling behavior during thermal conversion, as analyzed in the following section.

On a dry-ash-free (daf) basis, the material was dominated by volatile matter (86.7%) with a small, fixed carbon fraction (13.3%). The proximate composition of *Q. pubescens* bark is slightly different from that of other biomass types, with lower volatile content and elevated ash content [45]. The calorific value of 14.9 MJ/kg is moderate for a lignocellulosic residue and reflects the combined effects of high ash and extractive contents.

Table 7. Fuel properties *of Quercus pubescens* bark (B).

Proximate Composition (%)				
Basis	MC	Ash	VM	FC
As-received	7.8	16.3	65.8	10.1
Dry	0.0	17.7	71.4	10.9
Dry-ash-free	0.0	0.0	86.7	13.3
Calorific value (MJ/kg)	14.9			

3.4. Slagging and Fouling Risks

In the transition from fossil fuels to renewable energy, combustion of biomass is considered a carbon-neutral process. But it presents certain operational challenges. Contrary to coal, biomass combustion may create operational problems such as slagging and fouling because of its alkali (Na, K), chlorine, and silicon content [46–48]. Therefore, lower furnace temperatures are usually employed, combustion efficiency reduces, and maintenance requirement increases [48].

The ash melting (fusion) temperature (AFT) is the temperature range where the inorganic fraction of the solid fuel starts to deform, soften, and expand, becomes a hemisphere, and finally melts into a liquid slag (ASTM D1857 [49]). The characteristic ash melting temperatures of *Quercus pubescens* bark are shown in Table 8 and Figure 7.

Table 8. Ash melting temperatures of *Quercus pubescens* bark (B).

Stages	Preheat	Deformation	Softening	Hemisphere	Flow
Temperatures (°C)	698	1373	1421	1457	1476

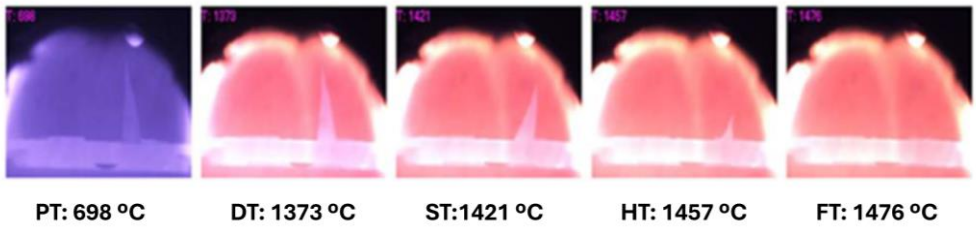


Figure 7. Ash melting temperatures of *Quercus pubescens* bark.

These results show that *Q. pubescens* ash has excellent thermal stability with a flow temperature of 1476 °C, which is higher than coal (1213 °C) [45] and different waste biomass such as alfalfa, straw, and hay [50]. It is not likely to slag during biomass combustion or coal-biomass co-combustion, which occurs below 1200 °C. The fouling risk is moderate to low with a deformation temperature of 1373 °C.

These results are in line with previous publications and show that CaO-based ashes have high melting points [51,52]. The very low iron, potassium, silicon, and sulfur contents of the bark did not reduce ash melting temperatures by forming low-melting eutectic mixtures.

Despite AFT values indicating a low slagging risk, the ash chemical composition still suggests some fouling potential, as the total alkali content (Na_2O + K_2O) reaches 1.2%. This level is not negligible and may contribute to deposit formation during combustion. In practice, the impact of fouling also depends on boiler design. Fire-tube boilers, where hot gases pass through tubes surrounded by water, are more tolerant because ash deposits

can be mechanically removed relatively easily. On the other hand, water-tube boilers, which operate at higher efficiencies but are more sensitive to fouling, would require stricter monitoring and more frequent cleaning to avoid fouling issues. Therefore, while *Q. pubescens* bark is suitable for combustion and gasification with low slagging risk, its modest fouling tendency should be considered when selecting and operating boiler systems.

The bark structural features have direct process implications for thermochemical transformation. During thermal conversion, calcium oxalate monohydrate undergoes a well-known decomposition sequence: dehydration and CO release to form $CaCO_3$ between 150 and 500 °C, followed by CO_2 release to form CaO between 600 and 800 °C [53]. This pathway explains the observed broad thermal degradation range (150–690 °C) and aligns with the measured high ash softening (1421 °C) and flow (1467 °C) temperatures, which indicate low slagging and fouling risk [51].

Moreover, the transformation of calcium oxalate monohydrate into CaO provides in situ basic catalytic sites that can promote tar cracking and reforming [54,55], thereby improving gas quality while sustaining a char yield of approximately 35%. The abundance of phenolic extractives possibly contributes to early devolatilization and secondary char formation [56]. Together, these results demonstrate that the mineral and chemical composition of *Q. pubescens* bark enhances its suitability for thermochemical biorefineries, where calcium-rich phases and phenolic constituents create synergistic pathways for energy, biochar, and ash valorization.

3.5. Techno-Ecological Pathways and Process Implications

The characterization of *Q. pubescens* bark demonstrates how material properties may affect thermochemical biorefineries. The dominance of calcium oxalate monohydrate governs ash chemistry and thermal decomposition pathways. Low activation energy (70 kJ/mol), stable ash behavior (softening at 1421 °C, flow at 1467 °C), and a char yield of approximately 35% highlight the bark's suitability for combustion and gasification with minimal slagging and moderate fouling risks. Within a techno-ecological framework, these process outputs also extend beyond energy: biochar and calcium-rich ash function as soil amendments, pH regulators, and carbon sinks, enabling their reintegration into managed soils. Association of biorefineries with soil management thus ensures that biomass valorization supports circular economy goals while reinforcing ecological services and resilient land-use systems.

The environmental co-benefits discussed herein are qualitative but directly supported by the measured physicochemical data, including activation energy, ash fusion behavior, and char yield. These parameters provide the necessary baseline for future quantitative assessments, such as life-cycle or carbon-footprint analyses to evaluate the broader techno-ecological advantages of utilizing *Quercus pubescens* bark in thermochemical biorefineries.

4. Conclusions

Quercus pubescens bark and bark fractions were analyzed for the first time with respect to their structural and chemical composition and potential use in thermochemical biorefineries. The following conclusions are derived from this study.

1. *Q. pubescens* bark contains a significant amount of phenolic extractives (21%) and inorganics (15%). The inorganic fraction of the bark is dominated by calcium oxalate, mainly in monohydrate form (COM).
2. Thermal degradation of the bark occurs between 150 °C and 690 °C. The ash softening temperature is 1421 °C, and the ash flow temperature is 1467 °C. The raw bark has a very low slagging risk and a moderate fouling risk.

3. Extractives enhance the bark thermal degradation by catalytic activity. Suberin decreases the thermal degradation by forming a physical barrier.
4. Reactivity analyses of bark fractions favor their different thermochemical biorefinery routing: extracted bark (EB) and desuberinised bark (DB) are highly reactive and well-suited to combustion/gasification, whereas raw bark (RB) and Klason lignin (KL) exhibit higher thermal stability and yield more persistent char
5. The proposed extraction and desuberinization steps were designed to demonstrate fraction-specific valorization routes rather than to define an optimized industrial process. Although such pre-processing would entail additional energy input at larger scales, these costs can potentially be offset through co-product valorization and process heat integration in future techno-economic and life-cycle assessments.
6. Although the high mineral and extractive content of *Q. pubescens* bark may limit direct pyrolysis efficiency compared with feedstocks with more polysaccharides and lignin, these same characteristics open opportunities for integrated process optimization. Targeted fractionation can convert these compositional constraints into functional advantages. Therefore, the present dataset provides a foundation for future process-integration and techno-economic studies aimed at overcoming these inherent limitations and enabling efficient utilization of tree barks in circular biorefineries.

Author Contributions: Conceptualization, U.Ş. and H.P.; methodology, U.Ş., I.M. and Ş.A.; formal analysis, B.B., Ş.A., B.Ş. and I.M.; investigation, U.Ş., B.B. and Ş.A.; resources, U.Ş.; writing—original draft preparation, U.Ş.; writing—review and editing, U.Ş., Ş.A., I.M., B.Ş. and H.P.; visualization, U.Ş. and H.P.; supervision, H.P. All authors have read and agreed to the published version of the manuscript.

Funding: This research received no external funding.

Data Availability Statement: The original contributions presented in this study are included in the article. Further inquiries can be directed to the corresponding author.

Acknowledgments: The authors thank Joaquina Silva, Isabel Nogueira, and Francisco Lemos from the University of Lisbon for their kind help in instrumental analysis. The authors would like to gratefully acknowledge the support of the Integrated Research Center (TAM) of Izmir Institute of Technology.

Conflicts of Interest: The authors declare no conflicts of interest.

Abbreviations

The following abbreviations are used in this manuscript:

AFT	Ash fusion temperatures
B	Bark
Csa	Hot-summer Mediterranean climate
DB	Desuberinised bark
DSC	Differential scanning calorimetry
EB	Extracted bark
EDS	Energy dispersive X-ray spectroscopy
FT-IR	Fourier-transform infrared spectroscopy
HHV	Higher heating value
HR	Heating rate
KL	Klason lignin
MC	Moisture content

SEM	Scanning electron microscopy
TGA	Thermogravimetric analysis
XRD	X-ray diffraction
XRF	X-ray fluorescence

Appendix A

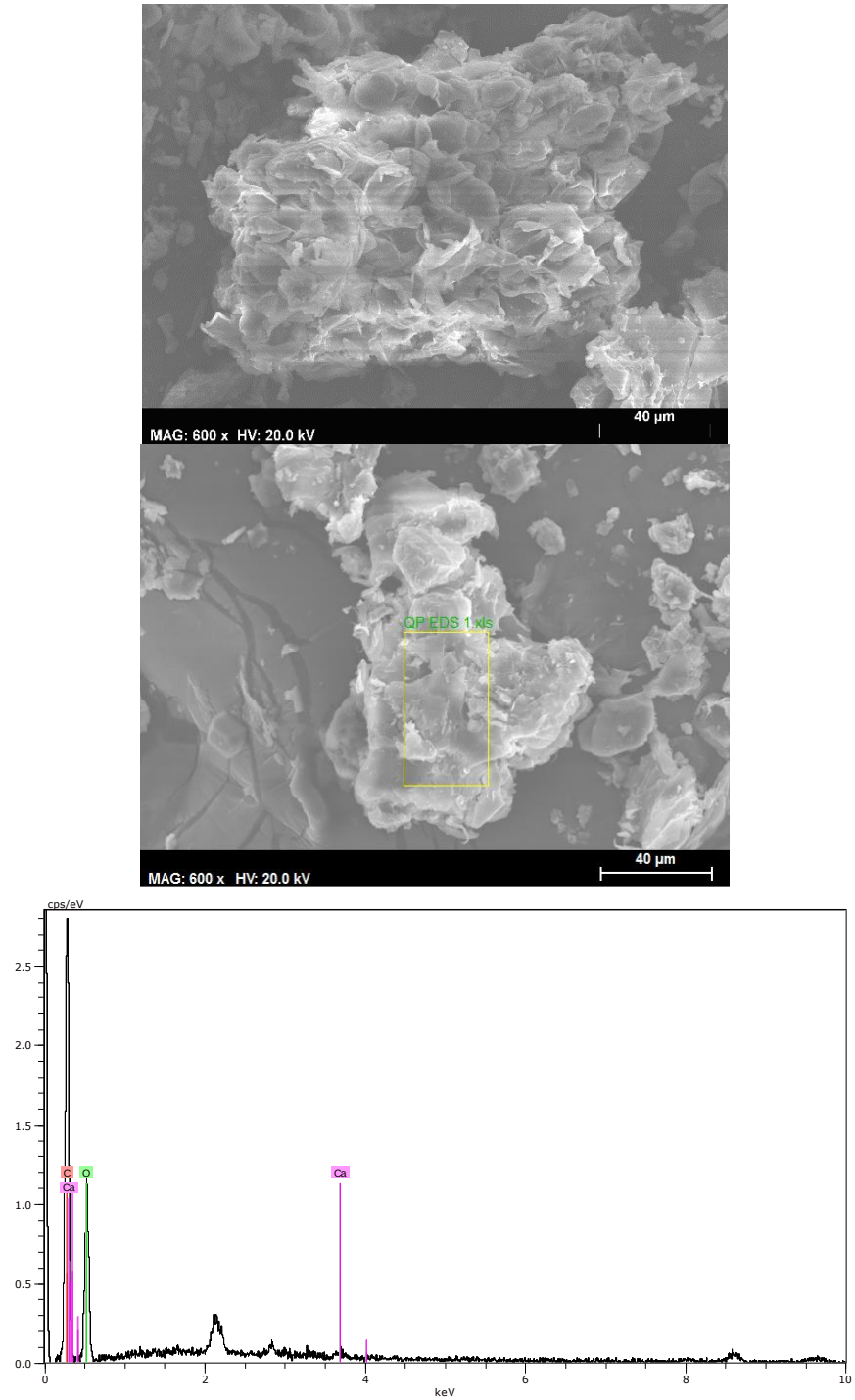
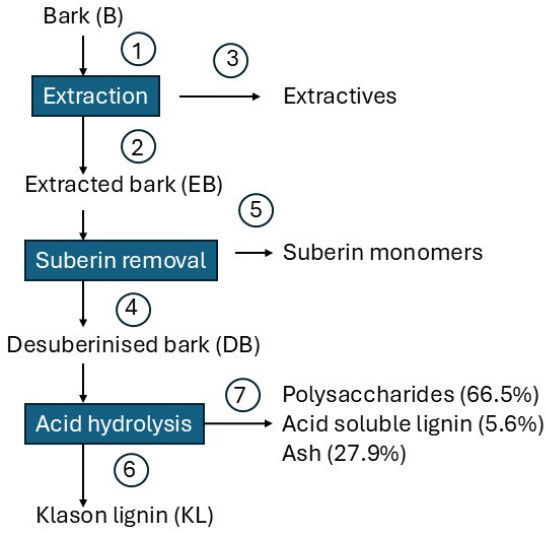


Figure A1. Bark structure of *Quercus pubescens* bark (**above**), analysis of EDS (**middle**), and EDS spectra (**below**) confirming the presence of calcium.



kg	1	2	3	4	5	6	7
B	**100**	-	-	-	-	-	
EB	-	**78.8**	21.2	-	-	-	
DB	-	-	-	**74.7**	4.1	-	
KL	-	-	-	-	-	**21.0**	53.7
Total	-	78.8	21.2	74.7	4.1	21.0	53.7

Figure A2. Fractionation of *Quercus pubescens* bark and mass balance table based on 100 kg bark. Klason lignin may contain acid-insoluble inorganic impurities.

References

1. Yaltırık, F. *Türkiye Meşeleri Teşhis Kılavuzu [Guide for Identification of Turkish Oaks]*; Tarım Orman ve Köyişleri Genel Müdürlüğü: İstanbul, Turkey, 1984.
2. Mévy, J.-P.; Loriod, B.; Liu, X.; Corre, E.; Torres, M.; Büttner, M.; Haguenauer, A.; Reiter, I.M.; Fernandez, C.; Gauquelin, T. Response of downy oak (*Quercus pubescens* Willd.) to climate change: Transcriptome assembly, differential gene analysis and targeted metabolomics. *Plants* **2020**, *9*, 1149. [CrossRef]
3. Pasta, S.; De Rigo, D.; Caudullo, G. Quercus Pubescens in Europe: Distribution, Habitat, Usage and Threats. In *European Atlas of Forest Tree Species*; Publications Office of the European Union: Luxembourg, 2016; pp. 156–157.
4. Kätzel, R. Die Vorkommen der Flaum-Eiche und ihrer Hybriden nördlich der Alpen. *Landbauforsch. Appl. Agric. For. Res.* **2014**, *64*, 73–84.
5. Todaro, L.; Rita, A.; Negro, F.; Moretti, N.; Saracino, A.; Zanuttini, R. Behavior of pubescent oak (*Quercus pubescens* Willd.) wood to different thermal treatments. *iForest* **2015**, *8*, 748–756. [CrossRef]
6. Davis, P.H. *Flora of Turkey and the East Aegean Islands*; University Press: Edinburgh, UK, 1982; Volume 7, pp. 672–673.
7. Di Pietro, R.; Di Marzio, P.; Antonecchia, G.; Conte, A.L.; Fortini, P. Preliminary characterization of the *Quercus pubescens* complex in southern Italy using molecular markers. *Acta Bot. Croat.* **2020**, *79*, 15–25. [CrossRef]
8. Lo Gullo, M.A.; Salleo, S. Wood anatomy of some trees with diffuse- and ring-porous wood: Some functional and ecological interpretations. *Plant Biosyst.* **1990**, *124*, 601–613. [CrossRef]
9. Humar, M.; Balzano, A.; Grbec, S.; Gričar, J.; Kržišnik, D.; Lesar, B.; Vek, V. Investigation of the material resistance and moisture performance of pubescent oak (*Quercus pubescens*). *Holzforschung* **2021**, *75*, 22–36. [CrossRef]
10. Moretti, N.; Bufo, S.A.; Fouilloux, C.; Lelario, F.; Capogrossi, A.; Sinisgalli, C.A.; Milella, L.; Scrano, L. Primi risultati sulla utilizzazione del legname di *Quercus pubescens* Willd. (roverella) per la produzione di botti da invecchiamento. *L'Italia For. Mont.* **2019**, *74*, 143–154. [CrossRef]
11. Miljić, U.; Puškaš, V.; Correia, A.C.; Jordão, A.M. The impact of *Quercus pubescens* wood chips on chemical and sensory characteristics of a Serbian 'Kadarka' red wine during aging: A comparison with other oak species (*Q. petraea*, *Q. alba*, and *Q. pyrenaica*). *Vitis* **2023**, *62*, 41–58. [CrossRef]
12. Nișca, A.; Ștefănescu, R.; Mocan, A.; Babotă, M.; Nicolescu, A.; Mare, A.D.; Ciurea, C.N.; Man, A.; Tănase, C. A comparative analysis of polyphenol content and biological potential of *Quercus petraea* Matt. and *Q. pubescens* Willd. bark extracts. *Forests* **2023**, *14*, 116. [CrossRef]
13. Vangeel, T.; Neiva, D.M.; Quilhó, T.; Costa, R.A.; Sousa, V.; Sels, B.F.; Pereira, H. Tree bark characterization envisioning an integrated use in a biorefinery. *Biomass Convers. Biorefin.* **2021**, *11*, 2029–2043. [CrossRef]
14. Le Normand, M.; Moriana, R.; Ek, M. The bark biorefinery: A side-stream of the forest industry converted into nanocomposites with high oxygen-barrier properties. *Cellulose* **2014**, *21*, 4583–4594. [CrossRef]
15. Neiva, D.M.; Araújo, S.; Gominho, J.; de Cássia Carneiro, A.; Pereira, H. Potential of *Eucalyptus globulus* industrial bark as a biorefinery feedstock: Chemical and fuel characterization. *Ind. Crops Prod.* **2018**, *123*, 262–270. [CrossRef]
16. Fengel, D.; Wegener, G. *Wood: Chemistry, Ultrastructure, Reactions*; Walter de Gruyter: Berlin, Germany; New York, NY, USA, 1984.

17. McBride, M.B.; Kelch, S.; Schmidt, M.; Zhou, Y.; Aristilde, L.; Martinez, C.E. Lead solubility and mineral structures of coprecipitated lead/calcium oxalates. *Environ. Sci. Technol.* **2019**, *53*, 13794–13801. [CrossRef] [PubMed]
18. *TAPPI T204 om-84*; Solvent Extractives of Wood and Pulp. TAPPI Press: Atlanta, GA, USA, 1987.
19. *TAPPI T207 om-93*; Water Solubility of Wood and Pulp. TAPPI Press: Atlanta, GA, USA, 1993.
20. Graça, J.; Pereira, H. Methanolysis of bark suberins: Analysis of glycerol and acid monomers. *Phytochem. Anal.* **2000**, *11*, 45–51. [CrossRef]
21. *TAPPI T222 om-88*; Acid Insoluble Lignin in Wood and Pulp. TAPPI Press: Atlanta, GA, USA, 1988.
22. *TAPPI UM 250*; Acid-Soluble Lignin in Wood and Pulp. TAPPI Press: Atlanta, GA, USA, 1991.
23. Sluiter, A.; Hames, B.; Ruiz, R.; Scarlata, C.; Sluiter, J.; Templeton, D.; Crocker, D. *Determination of Structural Carbohydrates and Lignin in Biomass (NREL LAP 1617)*; National Renewable Energy Laboratory: Golden, CO, USA, 2008.
24. Lu, J.-J.; Chen, W.-H. Investigation on the ignition and burnout temperatures of bamboo and sugarcane bagasse by thermogravimetric analysis. *Appl. Energy* **2015**, *160*, 49–57. [CrossRef]
25. Ding, Y.; Zhang, W.; Zhang, X.; Han, D.; Liu, W.; Jia, J. Pyrolysis and combustion behavior study of PMMA waste from micro-scale to bench-scale experiments. *Fuel* **2022**, *319*, 123717. [CrossRef]
26. *ASTM E871-82*; Standard Test Method for Moisture Analysis of Particulate Wood Fuels. ASTM International: West Conshohocken, PA, USA, 2019.
27. *ASTM E872-82*; Standard Test Method for Volatile Matter in the Analysis of Particulate Wood Fuels. ASTM International: West Conshohocken, PA, USA, 2019.
28. *ASTM D1102-84*; Test Method for Ash in Wood. ASTM International: West Conshohocken, PA, USA, 2008.
29. Lavrič, M.; Eler, K.; Ferlan, M.; Vodnik, D.; Gričar, J. Chronological sequence of leaf phenology, xylem and phloem formation and sap flow of Quercus pubescens from abandoned Karst grasslands. *Front. Plant Sci.* **2017**, *8*, 314. [CrossRef]
30. Trockenbrodt, M. Calcium oxalate crystals in the bark of *Quercus robur*, *Ulmus glabra*, *Populus tremula* and *Betula pendula*. *Ann. Bot.* **1995**, *75*, 281–284. [CrossRef]
31. Şen, A.; Marques, A.V.; Gominho, J.; Pereira, H. Study of thermochemical treatments of cork in the 150–400 °C range using colour analysis and FTIR spectroscopy. *Ind. Crops Prod.* **2012**, *38*, 132–138. [CrossRef]
32. Şen, A.U.; Simões, R.; Yücedağ, C.; Quilhó, T.; Sousa, V.; Miranda, I.; Fernandes, Â.; Pereira, H. Bark-based biorefineries: Anatomical and chemical characterization of the bark of endemic *Quercus vulcanica* of Turkey. *Wood Sci. Technol.* **2024**, *58*, 333–355. [CrossRef]
33. Maruyama, M.; Sawada, K.P.; Tanaka, Y.; Okada, A.; Momma, K.; Nakamura, M.; Mori, R.; Furukawa, Y.; Sugiura, Y.; Tajiri, R. Quantitative analysis of calcium oxalate monohydrate and dihydrate for elucidating the formation mechanism of calcium oxalate kidney stones. *PLoS ONE* **2023**, *18*, e0282743. [CrossRef] [PubMed]
34. French, A.D. Idealized powder diffraction patterns for cellulose polymorphs. *Cellulose* **2014**, *21*, 885–896. [CrossRef]
35. Wang, L.; Shen, Y. Pyrolysis characteristics of cellulosic biomass in the presence of alkali and alkaline-earth-metal (AAEM) oxalates. *Cellulose* **2021**, *28*, 3473–3483. [CrossRef]
36. Trubetskaya, A. Reactivity effects of inorganic content in biomass gasification: A review. *Energies* **2022**, *15*, 3137. [CrossRef]
37. Şen, U.; Esteves, B.; Pereira, H. Pyrolysis and extraction of bark in a biorefineries context: A critical review. *Energies* **2023**, *16*, 4848. [CrossRef]
38. Leite, C.; Pereira, H. Cork-containing barks—A review. *Front. Mater.* **2017**, *3*, 63. [CrossRef]
39. Şen, A.; Van den Bulcke, J.; Defoirdt, N.; Van Acker, J.; Pereira, H. Thermal behaviour of cork and cork components. *Thermochim. Acta* **2014**, *582*, 94–100. [CrossRef]
40. Fetisova, O.Y.; Mikova, N.M.; Chudina, A.I.; Kazachenko, A.S. Kinetic study of pyrolysis of coniferous bark wood and modified fir bark wood. *Fire* **2023**, *6*, 59. [CrossRef]
41. Qian, L. Influence of extractives on mechanism of biomass pyrolysis. *J. Fuel Chem. Technol.* **2010**, *38*, 42–46. [CrossRef]
42. Wang, Z.; Zhao, Z.; Qian, J. Effects of extractives on degradation characteristics and VOCs released during wood heat treatment. *BioResources* **2020**, *15*, 211–226. [CrossRef]
43. Ren, X.; Guo, J.; Li, S.; Chang, J. Thermogravimetric analysis–Fourier transform infrared spectroscopy study on the effect of extraction pretreatment on the pyrolysis properties of Eucalyptus wood waste. *ACS Omega* **2020**, *5*, 23364–23371. [CrossRef] [PubMed]
44. Weiland, F.; Lundström, S.; Ögren, Y. Oxygen-blown gasification of pulp mill bark residues for synthetic fuel production. *Processes* **2021**, *9*, 163. [CrossRef]
45. Fang, X.; Jia, L. Experimental study on ash fusion characteristics of biomass. *Bioresour. Technol.* **2012**, *104*, 769–774. [CrossRef] [PubMed]
46. Lachman, J.; Baláš, M.; Lisý, M.; Lisá, H.; Milčák, P.; Elbl, P. An overview of slagging and fouling indicators and their applicability to biomass fuels. *Fuel Process. Technol.* **2021**, *217*, 106804. [CrossRef]

47. Li, Q.H.; Zhang, Y.G.; Meng, A.H.; Li, L.; Li, G.X. Study on ash fusion temperature using original and simulated biomass ashes. *Fuel Process. Technol.* **2013**, *107*, 107–112. [CrossRef]
48. Yang, Z.; Li, F.; Ma, M.; Liu, X.; Fan, H.; Li, Z.; Wang, Y.; Fang, Y. Regulation mechanism of solid waste on ash fusion characteristics of sorghum straw under O_2/CO_2 atmosphere. *Energies* **2023**, *16*, 7052. [CrossRef]
49. *ASTM D1857*; Standard Test Method for Fusibility of Coal and Coke Ash. ASTM International: West Conshohocken, PA, USA, 2024.
50. Čajová Kantová, N.; Holubčík, M.; Trnka, J.; Čaja, A. Analysis of ash melting temperatures of agricultural pellets detected during different conditions. *Fire* **2023**, *6*, 88. [CrossRef]
51. Liang, W.; Wang, G.; Ning, X.; Zhang, J.; Li, Y.; Jiang, C. Effect of CaO mineral change on coal ash melting characteristics. *J. Energy Inst.* **2020**, *93*, 642–648. [CrossRef]
52. Bgasheva, T.; Falyakhov, T.; Petukhov, S.; Sheindlin, M.; Vasin, A.; Vervikishko, P. Laser-pulse melting of calcium oxide and some peculiarities of its high-temperature behavior. *J. Am. Ceram. Soc.* **2021**, *104*, 3461–3477. [CrossRef]
53. Lawson-Wood, K.; Robertson, I. Study of the Decomposition of Calcium Oxalate Monohydrate Using a Hyphenated Thermogravimetric Analyser–FT-IR System (TG-IR). PerkinElmer Application Note. 2016. Available online: https://www.s4science.at/wordpress/wp-content/uploads/2018/10/TL8000-TG-IR-Decomposition-Calcium-Oxalate-Monohydrate-Application-Note.pdf (accessed on 1 August 2025).
54. Wang, J.; Zhao, B.; Zhu, D.; Huang, F.; Zhang, W.; Yang, H.; Chen, L.; Guan, H.; Sun, L.; Yang, S. Mechanism on catalytic cracking tar with CaO-based catalysts for hydrogen-rich gas by DFT and experiments. *Int. J. Hydrogen Energy* **2021**, *46*, 6522–6531. [CrossRef]
55. Zhou, L.; Yang, Z.; Tang, A.; Huang, H.; Wei, D.; Yu, E.; Lu, W. Steam-gasification of biomass with CaO as catalyst for hydrogen-rich syngas production. *J. Energy Inst.* **2019**, *92*, 1641–1646. [CrossRef]
56. Carrier, M.; Windt, M.; Ziegler, B.; Appelt, J.; Saake, B.; Meier, D.; Bridgwater, A. Quantitative insights into the fast pyrolysis of extracted cellulose, hemicelluloses, and lignin. *ChemSusChem* **2017**, *10*, 3212–3224. [CrossRef]

Disclaimer/Publisher's Note: The statements, opinions and data contained in all publications are solely those of the individual author(s) and contributor(s) and not of MDPI and/or the editor(s). MDPI and/or the editor(s) disclaim responsibility for any injury to people or property resulting from any ideas, methods, instructions or products referred to in the content.